

Ultrathin nucleoporin phenylalanine–glycine repeat films and their interaction with nuclear transport receptors

Nico B. Eisele^{1,2}, Steffen Frey², Jacob Piehler³, Dirk Görlich² & Ralf P. Richter^{1,4*}

¹Biosurfaces Unit, Centre for Cooperative Research in Biomaterials, Donostia—San Sebastian, Spain, ²Department of Cellular Logistics, Max Planck Institute for Biophysical Chemistry, Göttingen, Germany, ³Department of Biology, University of Osnabrück, Osnabrück, Germany, and ⁴Max Planck Institute for Metals Research, Stuttgart, Germany

 This is an open-access article distributed under the terms of the Creative Commons Attribution License, which permits distribution, and reproduction in any medium, provided the original author and source are credited. This license does not permit commercial exploitation without specific permission.

Nuclear pore complexes (NPCs) are highly selective gates that mediate the exchange of all proteins and nucleic acids between the cytoplasm and the nucleus. Their selectivity relies on a supramolecular assembly of natively unfolded nucleoporin domains containing phenylalanine–glycine (FG)-rich repeats (FG repeat domains), in a way that is at present poorly understood. We have developed ultrathin FG domain films that reproduce the mode of attachment and the density of FG repeats in NPCs, and that exhibit a thickness that corresponds to the nanoscopic dimensions of the native permeability barrier. By using a combination of biophysical characterization techniques, we quantified the binding of nuclear transport receptors (NTRs) to such FG domain films and analysed how this binding affects the swelling behaviour and mechanical properties of the films. The results extend our understanding of the interaction of FG domain assemblies with NTRs and contribute important information to refine the model of transport across the permeability barrier.

Keywords: FG repeat domain; nuclear pore complex; nuclear transport receptor; nucleoporins; permeability barrier

EMBO reports (2010) 11, 366–372. doi:10.1038/embor.2010.34

¹Biosurfaces Unit, Centre for Cooperative Research in Biomaterials, Paseo Miramon 182, Donostia—San Sebastian 20009, Spain

²Department of Cellular Logistics, Max Planck Institute for Biophysical Chemistry, Am Fassberg 11, Göttingen 37077, Germany

³Department of Biology, University of Osnabrück, Barbarastrasse 11, Osnabrück 49076, Germany

⁴Max Planck Institute for Metals Research, Heisenbergstrasse 3, Stuttgart 70569, Germany

*Corresponding author. Tel: +34 943 00 5329; Fax: +34 943 00 5315; E-mail: rrichter@cicbiomagune.es

Received 27 August 2009; revised 28 January 2010; accepted 12 February 2010; published online 9 April 2010

INTRODUCTION

All eukaryotic cells rely on nuclear pore complexes (NPCs) as the unique path to shuttle macromolecules across their nuclear envelope. Translocation through the central channel, with a diameter and length of 35–40 nm in the case of yeast (Yang *et al*, 1998), is selective: molecules smaller than 5 nm in diameter (Mohr *et al*, 2009) can diffuse efficiently through the pore, whereas larger molecules are delayed or blocked—unless they are bound to nuclear transport receptors (NTRs). The permeability barrier, and its selectivity, arises from an assembly of natively unfolded protein domains that are rich in phenylalanine–glycine repeats (FG repeat domains; Denning *et al* (2003) and references therein) and that are grafted at a high density on to the channel walls. These NTRs can interact with the FG repeat domains, thereby facilitating the translocation of NTR-bound cargo.

Several models have been proposed to explain the mechanism of function of the permeability barrier (Peters, 2009, and references therein). They are distinct in the putative nanoscale organization of FG repeats and in how NTRs are thought to interact with FG repeats to confer selective permeability to such a dynamic supramolecular assembly. In the ‘virtual gating’ (Rout *et al*, 2003) and ‘selective phase’ (Ribbeck & Görlich, 2001, 2002) models, for example, NTRs are thought to interact locally with a homogeneous distribution of FG repeat domains. The ‘reversible collapse’ model (Lim *et al*, 2007), by contrast, assumes transient morphological changes over distances as large as the contour length of entire FG repeat domains. The ‘reduction of dimensionality’ (Peters, 2005) model postulates the presence of a distinct structure, a surface lined with FG repeats, for efficient translocation of NTRs.

Inspired by these models, we sought to create *in vitro* nanoscopic assemblies of FG repeat domains to provide detailed insight into the interaction between NTRs and FG repeat-domain meshworks, and the concomitant morphological changes that are

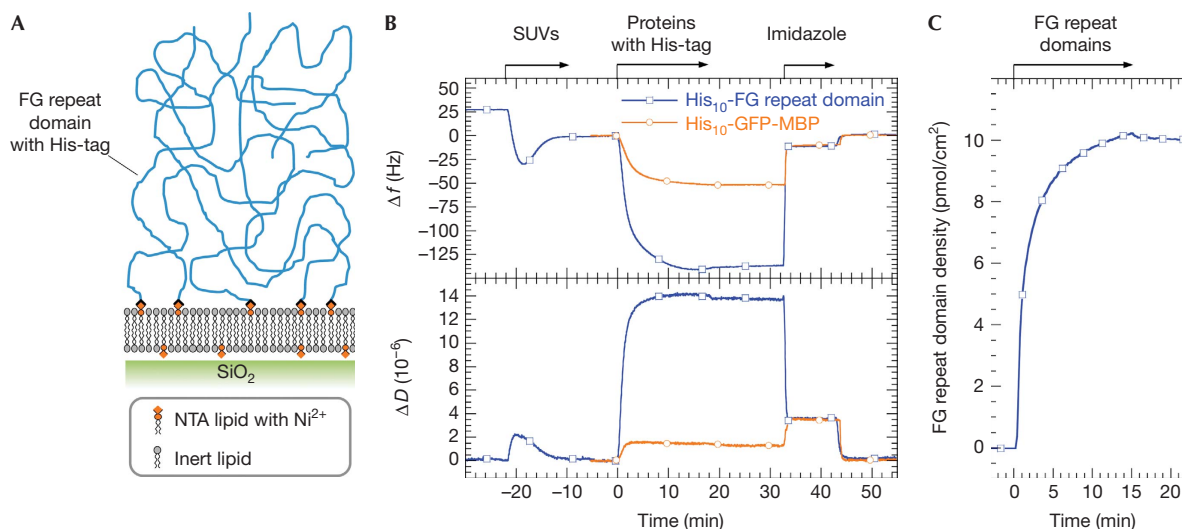


Fig 1 | Formation of membrane-anchored monolayers of phenylalanine-glycine repeat domains. (A) Scheme illustrating the film architecture. The FG repeat domain of Nsp1p (amino acids 2–601) was grafted through an amino-terminal His₁₀ tag to a bis-NTA-functionalized SLB. (B) Construction of an FG repeat film, followed by quartz crystal microbalance with dissipation monitoring. The start and duration of the incubation with different samples is indicated (arrows); remaining times correspond to buffer washes. The SLB was formed by exposure of 50 μg/ml SUVs, containing 10 mol% bis-NTA-functionalized lipids, to a silica surface. The two-phase behaviour together with the final changes in frequency and dissipation, $\Delta f = -28$ Hz and $\Delta D < 0.3 \times 10^{-6}$, characterize the formation of an SLB of good quality. Strong changes in frequency and dissipation on the addition of 1.5 μM His-tagged FG repeat domains reflect the formation of a flexible and hydrated film. Binding of 1.4 μM His-tagged GFP-MBP is shown for comparison. This fusion of globular proteins with a comparable molecular weight and an identical His-tag to the FG repeat domains induced about one-third of the frequency shift of the FG repeats and a low dissipation shift, as expected for a rigid monolayer of about 8 nm in thickness. At the end of the film formation processes, $\Delta D/\Delta f$ ratios of 0.1×10^{-6} /Hz for FG repeat domains and 0.028×10^{-6} /Hz for GFP-MBP were reached. The more than threefold higher value for FG repeat domains reflects the increased softness of this film. All His-tagged proteins bound with high affinity but could be removed by washing with 500 mM imidazole. Changes in Δf and ΔD at about 43 min do not reflect any changes on the surface but result from a change in the viscosity or density of the surrounding solution owing to the presence of imidazole. (C) Ellipsometric analysis of the FG repeat domain density during film formation, with 3 μM His-tagged FG repeat domains in solution. FG, phenylalanine-glycine; GFP, green fluorescent protein; MBP, maltose-binding protein; NTA, nitrilotriacetic acid; SLB, supported lipid bilayer; SUV, small unilamellar vesicle.

induced by NTRs. We found continuous planar monolayers of end-grafted FG repeat domains (Fig 1A) to be suitable for this goal. Their macroscopic extension in two dimensions and their confinement to a solid support make such films amenable to characterization by surface-sensitive biophysical methods. By using such methods, the construction and morphology of the films can be controlled tightly and their interaction with NTRs quantified.

RESULTS AND DISCUSSION

Formation of FG repeat-domain films

We used supported lipid bilayers (SLBs; Richter *et al*, 2006) as a platform for the construction of FG repeat-domain films (Fig 1A). The SLBs provide a tuneable density of anchorage sites—here 10 mol% of bis-nitrilotriacetic-acid (NTA)-functionalized lipids (Lata *et al*, 2006)—together with a background of low unspecific binding. A His-tagged construct of the FG repeat domain (amino acids 2–601) of Nsp1p, a yeast nucleoporin that is essential for viability and located in the central region of the pore channel, was used as building material for the model films.

Step-by-step assembly of the films was monitored by quartz crystal microbalance with dissipation monitoring (QCM-D; Fig 1B). Strong shifts in resonance frequency, Δf , and dissipation,

ΔD , on incubation of the FG repeat construct provide evidence for successful formation of a soft and hydrated film. The FG repeat domains remained stably bound upon rinsing in buffer. They could be fully eluted with imidazole and did not bind to SLBs that lacked NTA functionality (supplementary Fig S5 online), indicating specific anchorage through their amino-terminal His tags. This ‘end on’ attachment is reminiscent of the anchorage of FG repeat domains to the NPC channel walls, although the orientation is upside down. The thickness of the film, 34 ± 4 nm, estimated from QCM-D data (supplementary Fig S2 online and supplementary Table S2 online), represents only a fraction of the contour length of the FG repeat domain (~ 250 nm) but is similar to the dimensions of the central NPC channel. We note that an FG repeat monolayer of such a thickness would readily fill the cross-section of the central NPC channel. Imaging by atomic force microscopy (AFM; supplementary Fig S4 online) revealed the surface of the film to be flat, indicating that the film is laterally homogeneous, at least, down to a length scale of a few 10 nm.

Adsorbed amounts were quantified by ellipsometry (Fig 1C; supplementary Fig S3 online). The final film density of 10.0 ± 0.5 pmol FG repeat domains per cm² corresponds to a mean distance of 4.4 ± 0.1 nm between neighbouring anchor points. By adjusting the incubation time for FG repeat domains,

lower and higher anchor densities could be achieved readily (data not shown). With each FG repeat domain of Nsp1p containing 36 FG repeat units, the surface density corresponds to an average concentration of 106 ± 18 mM FG repeat units inside the film. For comparison, we expect a similar repeat density in yeast NPC, when assuming that its approximately 3,500 FG repeat units (Strawn *et al.*, 2004) fill a volume that extends slightly beyond the boundaries of the pore channel, covering a total distance of about 50 nm along the channel axis. The FG repeat concentration is also comparable to macroscopic, *in vitro*-assembled FG repeat hydrogels that were shown recently to exhibit a selectivity of transport similar to that of intact NPCs (Frey & Görlich, 2007, 2009).

Binding of NTRs to FG repeat-domain films

Having established that our model films match the thickness, the FG repeat concentration and the 'end on' mode of chain attachment that are pertinent to NPCs, we considered how NTRs interact with such FG repeat meshworks. Ellipsometric assays (Fig 2A) with a selected NTR, importin- β from *Saccharomyces cerevisiae* (sclmp β /Kap95p), revealed binding in a concentration-dependent manner. The titration data (Fig 2D) could not be fitted well by a single Langmuir isotherm (data not shown), indicating that the film contains more than one type of binding site. The simplest model providing a good fit was a two-component Langmuir isotherm (Fig 2D), with apparent dissociation constants of $K_D^{(1)} = 0.32 \mu\text{M}$ and $K_D^{(2)} = 5.3 \mu\text{M}$ (Table 1). One might be tempted to attribute these dissociation constants to two discrete types of binding site. Our findings are, however, also consistent with the presence of a spectrum of binding sites that cover a range of affinities. We note that the lower dissociation constant is remarkably similar to those reported previously for the interaction of sclmp β (Pyhtila & Rexach, 2003) or mammalian Imp β (Ben-Efraim & Gerace, 2001) with FG Nups from the central region of the NPC. It should also be noted that the dissociation constants are unlikely to reflect the binding strength between NTRs and individual FG repeat units. Rather, they are the result of multivalent interactions.

Assuming independent binding sites, the two-component Langmuir isotherm predicts a saturation limit of 4.0 ± 0.4 pmol/cm², which is 2.5-fold less than the concentration of FG repeat domains, or about 90-fold less than the concentration of FG repeat units in the film. Given that Imp β has about nine binding sites for FG repeat units (Isgro & Schulten, 2005), this number suggests that the binding capacity of the film for NTRs is not limited by the concentration of FG motifs. We propose that volume exclusion and entropic effects are the limiting parameters.

Our experimental approach also enabled—for the first time, to the best of our knowledge—the quantification of the effect of Gsp1p•GTP, the yeast homologue of RanGTP, and cargo on NTR binding close to equilibrium (Fig 2; Table 1). Titration data for sclmp β •Gsp1p•GTP could be fitted well by using a simple Langmuir isotherm, and revealed a tenfold-increased dissociation constant as compared with $K_D^{(1)}$ for sclmp β alone, in qualitative agreement with earlier studies on various FG Nups (Allen *et al.*, 2001; Ben-Efraim & Gerace, 2001). By contrast, binding was enhanced 3–5-fold when sclmp β was in complex with a model cargo, a fusion protein made of a nuclear import signal and monomeric enhanced

green fluorescent protein (importin- β -binding domain (amino acids 2–63) of yeast Srp1p–mEGFP; sclImp β •IBB–mEGFP). We suggest that an allosteric mechanism enhances the docking of the cargo complex to FG repeats, and thereby counteracts the repulsion of large cargoes by the permeability barrier (Ribbeck & Görlich, 2002).

The binding of NTR was fast and fully reversible, except for sclmp β •Gsp1p•GTP, for which a minor fraction (<20%) remained bound after rinsing. The latter might reflect some tendency of the complex to precipitate at the high concentrations reached in the FG repeat film, and as a result, the determined affinity might represent a slight overestimate. The relaxation times for reaching binding equilibria were similar to the resolution of our experimental setup, which provides a lower bound of 0.1/s for the off-rates (Fig 2A–C; Table 1). Off-rates of the same order of magnitude have already been reported (Rabut *et al.*, 2004). We note that the intrinsic off-rates could be considerably higher, as mass transport to and from the surface is likely to limit the binding reaction (supplementary information online). Control experiments with an inert probe (maltose-binding protein–mCherry) on FG repeat films and with sclmp β on both FG repeat-free SLBs and films of FG/FxFG repeat domains, in which all phenylalanines in the FG context have been replaced by serines, confirmed that the assays are specific for the interaction of NTRs with the film (supplementary Figs S6–S8 online).

NTRs can permeate FG repeat-domain films

To test whether the NTR can travel across FG repeat-domain films, we doped SLBs with an additional functionality of 2% biotinylated lipids and immobilized a submonolayer (~ 1.4 pmol/cm²) of avidin on the SLB (Bingen *et al.*, 2008) before forming an FG repeat film (Fig 3). The film was affected only marginally by the presence of avidin: the FG repeat mass was reduced by less than 5% (data not shown) and non-biotinylated sclmp β bound in similar amounts (Fig 3B). Noticeably, biotinylated sclmp β showed increased binding, with saturation levels reached at similar times. The additional fraction of biotinylated NTR, about 0.5 pmol/cm², remained irreversibly bound, presumably by docking to the surface-immobilized avidin. These observations provide evidence that sclmp β could not only bind to but also efficiently permeate the FG repeat film.

Effect of NTR influx on the morphology of FG repeat films

The NTR-induced structural changes in FG repeats have been suggested to explain the transport selectivity of NTRs (Lim *et al.*, 2007; Peters, 2009), and we sought to characterize the effect of sclmp β influx on the morphology of the FG repeat film by AFM. Controlled indentation of FG repeat films with a nanoscopic probe (Fig 4A) revealed a repulsive interaction over a range of 30–40 nm, in agreement with the film thickness inferred from QCM-D. Interestingly, the presence of 1 μM sclmp β in solution, or about 0.5 mM in the film, did not significantly change the onset of repulsion and the shape of the force–distance curve (Fig 4A), indicating that sclmp β does not markedly affect the thickness and mechanical properties of the film. This finding was corroborated by supplementary QCM-D measurements covering a large range of NTR solution concentrations (Fig 4B). The QCM-D data are consistent with a minor increase in the thickness of the film, by a few nanometres, and a moderate increase in its rigidity

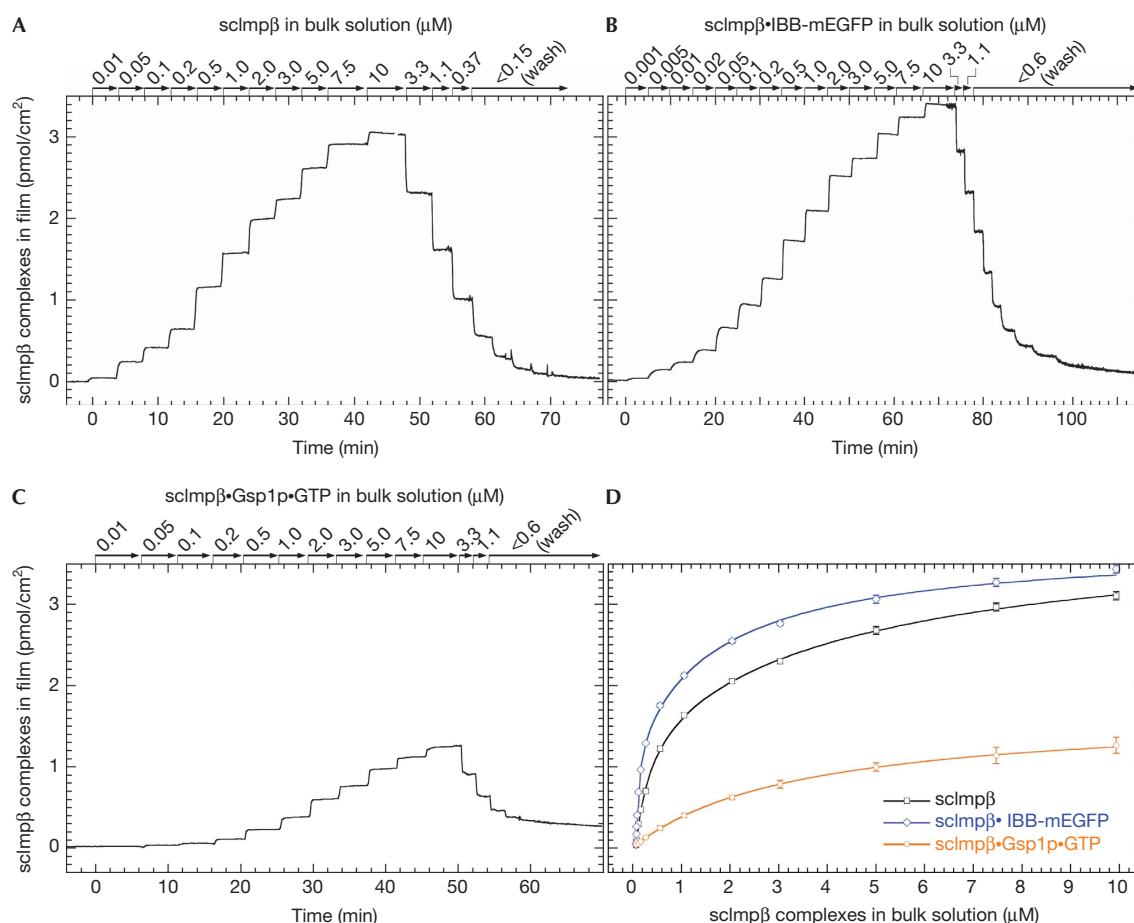


Fig 2 | Interaction of a nuclear transport receptor with phenylalanine-glycine repeat-domain films. Titration curves, determined by ellipsometry, for the binding of (A) free scImpβ, (B) scImpβ•IBB-mEGFP and (C) scImpβ•Gsp1p•GTP (in the presence of 100 μM excess GTP) to FG repeat films. (D) Absorbed amounts of scImpβ and its complexes at the equilibrium, with fits (solid lines) by single (scImpβ•Gsp1p•GTP) or two-component Langmuir isotherms (scImpβ, scImpβ•IBB-mEGFP). FG, phenylalanine-glycine; mEGFP, monomeric enhanced green fluorescent protein.

Table 1 | Binding parameters for the interaction of scImpβ and its complexes with phenylalanine-glycine repeat films

	$K_D^{(1)}$ (μM)	$K_D^{(2)}$ (μM)	$\Gamma_{max}^{(1)}$ (pmol/cm ²)	$\Gamma_{max}^{(2)}$ (pmol/cm ²)	Γ_{max}^{total} (pmol/cm ²)	PC (10 ³)	k_{off} (per s)
scImpβ	0.32 ± 0.04	5.3 ± 1.7	1.6 ± 0.2	2.4 ± 0.2	4.0 ± 0.4	1.5 ± 0.6	> 0.1
scImpβ•IBB-mEGFP	0.057 ± 0.004	1.8 ± 0.2	1.29 ± 0.06	2.40 ± 0.06	3.69 ± 0.12	6.7 ± 1.6	> 0.1
scImpβ•Gsp1p•GTP	3.5 ± 0.5	—	1.63 ± 0.13	—	1.63 ± 0.13	0.14 ± 0.05	> 0.1

mEGFP, monomeric enhanced green fluorescent protein; PC, partition coefficient.

(supplementary Table S2 online). Importantly, they firmly exclude a collapse of the film.

Implications for permeability barrier function

Binding of scImpβ considerably increases the total protein mass of the film. At 10 μM scImpβ level in solution, which approximates the total cellular NTR concentration (U. Jäkle and D.G., unpublished observations), the mass increases by about 45%. It might at first seem surprising that such a massive influx barely affects the thickness of the film. Our finding can be rationalized, however, by

simple arguments related to the physical behaviour of flexible polymers that are either crosslinked transiently or are entangled (polymer meshworks). With an approximate 100 mM FG repeat density, the FG repeat film contains on average about 12 FG repeat units within a volume that is occupied by a single scImpβ molecule. By contrast, not more than nine FG-binding sites have so far been suggested for mammalian Impβ (Isgro & Schulten, 2005). The NTR would thus find enough FG repeat units in the volume it displaces to saturate its binding sites. Recruitment of FG repeats from a distance is therefore not required, and a

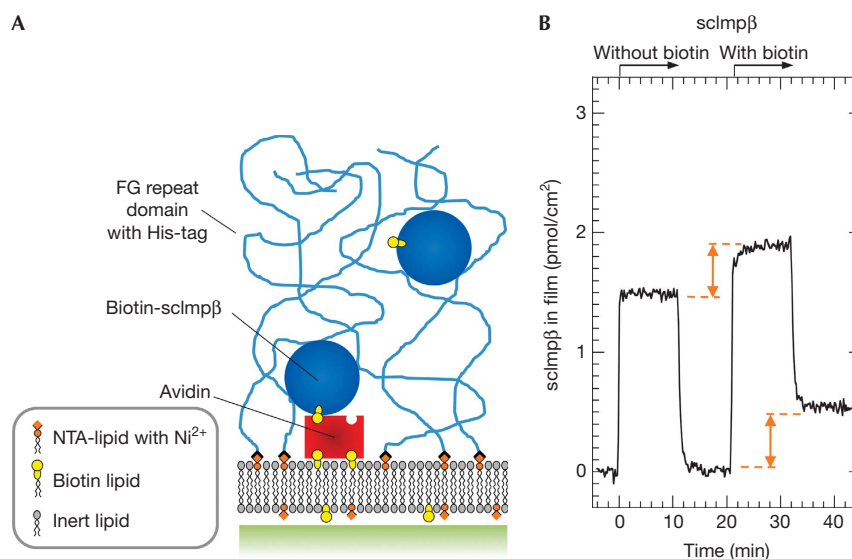


Fig 3 | Nuclear transport receptors can permeate phenylalanine-glycine repeat-domain films. (A) To assay permeation, SLBs were doped with an additional functionality of 2 mol% biotinylated lipids, and a submonolayer of avidin (1.4 pmol/cm^2) was immobilized on the SLB before the FG repeat-domain film was formed (data not shown). The size of the globular proteins (also see supplementary Fig S10 online) and the thickness of the SLB and the FG repeat film are drawn to scale. (B) Binding assay by ellipsometry: adsorption of $1 \mu\text{M}$ tag-free scImp β was fully reversible and similar in magnitude as in Fig 2. The same concentration of biotin-tagged scImp β exhibited significantly enhanced binding. The additional binding (indicated in orange) was irreversible. FG, phenylalanine-glycine; NTA, nitrilotriacetic acid; SLB, supported lipid bilayer.

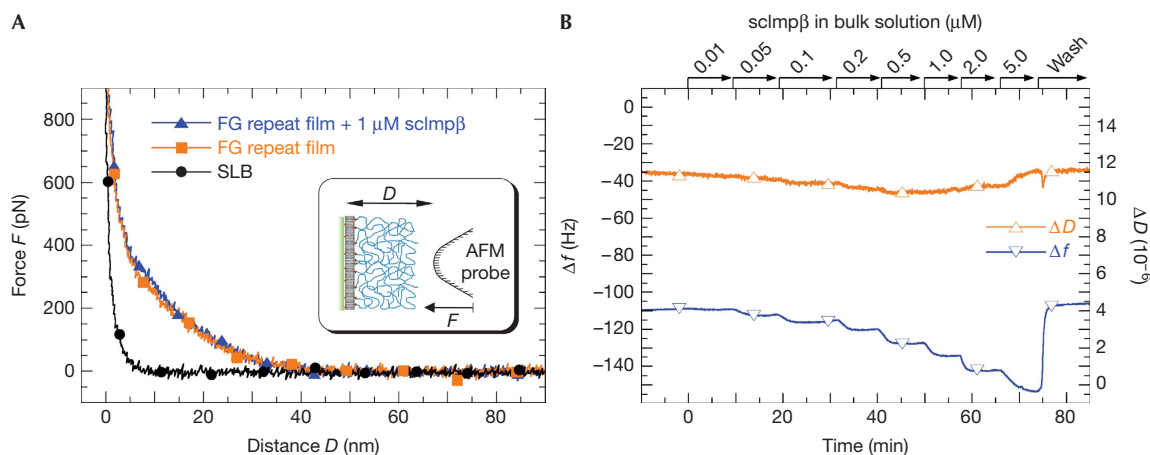


Fig 4 | Nuclear transport receptors moderately increase the thickness and rigidity of dense phenylalanine-glycine repeat films. (A) AFM indentation assay on FG repeat-domain films (schematic inset). Repulsive forces were detectable on FG repeat-domain films up to distances of 30–40 nm from the hard-wall compression limit. The onset of repulsion and the shape of the force–distance curve did not change significantly in the presence of $1 \mu\text{M}$ scImp β in the solution. Controls on SLB-covered silica before and after the indentation assay demonstrate that the interaction of these surfaces with the AFM probe remained rather short-ranged (around 6 nm). (B) The titration curve, measured by quartz crystal microbalance with dissipation monitoring, provides information about the changes in the mechanical properties of the film on scImp β binding. Changes in dissipation were small ($<10\%$ of the FG repeat film), whereas the changes in frequency were considerable ($\sim 45\%$ at $5 \mu\text{M}$). These data are consistent with a minor increase in the thickness of the film and a moderate increase in its rigidity, but exclude a collapse of the film (supplementary Table S2 online). AFM, atomic force microscopy; FG, phenylalanine-glycine; SLB, supported lipid bilayer.

collapse of the film is unlikely. At the same time, the inclusion of scImp β would require some FG repeat chains to be displaced from the volume that it occupies. The concomitant increase in film

thickness would at most correspond to the total added protein volume. Using a molecular volume of scImp β of 200 nm^3 and a surface density of 3.1 pmol/cm^2 , this thickness increase amounts

to approximately 4 nm. Film swelling would hence be moderate at best, consistent with our experiments.

This simple consideration of the physical behaviour of polymer meshworks has two notable implications. First, as it is not based on any details of the molecular structure of sclmp β , it is likely to apply to many, if not all, NTRs. Second, it predicts that on entering an FG repeat meshwork, NTRs would affect only their immediate environment, whereas more distant meshwork regions would remain unaffected. We suggest that such a separation of local and global morphology is important for the selectivity of the permeability barrier of the NPC. It allows two apparently contradictory functions to be accomplished simultaneously: local interactions between the NTR and FG repeats promote efficient translocation, while the rest of the permeability barrier remains unaffected and can continuously block inert molecules of similar size. This conjecture is consistent with both the 'virtual gating' and the 'selective phase' models.

The data obtained in our experimental setup, however, contrast with those described by Lim *et al* (2007), who reported a more than twofold decrease in thickness, from 30 nm down to 13 nm, on incubation of nanoscale islands of FG repeat meshworks with mammalian Imp β . On the basis of the argumentation above, such a collapse would only be plausible if the number of FG repeats available in the immediate environment of an approaching NTR is too small to saturate all of its FG repeat binding sites and if the interaction between NTR and FG repeats is sufficiently strong. Indeed, Lim *et al* (2007) used Nup153, a nucleoporin that is located in the nucleoplasmic region of the NPC and that exhibits an affinity for mammalian Imp β , which is at least one order of magnitude higher (Ben-Efraim & Gerace, 2001; Bednenko *et al*, 2003) than what is encountered typically for nucleoporins in the central region. Furthermore, estimates provided by Lim *et al* (2006) suggest that the density of FG repeat domains on the nanoscale islands was 5–30 times lower than in our study. We note that Lim *et al* (2007) found considerable collapse at a bulk concentration of 0.1 pM Imp β , several orders of magnitude below the affinity of Nup153 for Imp β (~ 10 nM) and the total cellular NTR concentration (~ 10 μ M). The discrepancy could be explained by direct binding of Imp β to the nanoscale gold islands to which the terminal cysteines of Nup153 FG repeat domains had been bonded. In such a case, it would not be surprising that the FG repeat domains appear collapsed while bound to surface-immobilized receptor molecules. This interpretation is supported by the fact that Imp β contains 23 cysteines and that excess binding sites on the gold islands had not been quenched in that study.

On the basis of our experimental findings and the average density of FG repeats in the NPC, we conclude that a 'nanomechanical collapse' is unlikely to occur in the central region of the NPC. Its noteworthy that the density of FG repeats is not homogeneous but might tend to decrease towards the peripheral regions of the NPC. Thus, at present, we cannot exclude the possibility that NTRs might affect the morphology of FG repeat domains at the boundary of the NPC. We stress that our data, and considerations of the behaviour of polymer meshworks, suggest that efficient entry, permeation and exit of NTRs can be accomplished without invoking any specific structures and pathways, such as a narrow tube along the axis of the NPC or channel walls, as required in some of the existing transport models (Macara, 2001; Peters, 2009).

Conclusions and Perspectives

Despite their simplicity in concept and composition, our model films provided hitherto inaccessible insight into the structure–function interrelationship of FG repeat-rich nucleoporin assemblies. Their two-dimensional extension made the FG repeat films accessible to label-free and quantitative analysis by a toolbox of surface-sensitive biophysical methods. We observed that sclmp β can efficiently enter, permeate and leave FG repeat films, and quantified the impact of cargo and Gsp1p•GTP on binding. Correlation of the binding of NTRs with concomitant changes in the swelling behaviour and mechanical properties of the FG repeat films revealed that the presence of sclmp β does not affect the global morphology of the FG repeat assemblies. This finding can be explained plausibly if we assume that the FG repeat domains form a dense meshwork, either cross-linked transiently or entangled, as postulated by the 'selective phase' model.

Our methodological approach can easily be extended to other FG repeats, or mixtures of them, and thus provides a simple tool for the screening of interactions with NTRs in a relevant and well-controlled nano-environment. Future studies will aim, in particular, at understanding the role of inter-FG repeat interactions in selective transport and at elucidating the parameters that govern the exclusion of inert or weakly interacting molecules from translocation.

METHODS

See the supplementary information online for materials, expression and purification of proteins, substrate preparation, the details of the implementation of QCM-D, ellipsometry, AFM indentation assays and imaging.

QCM-D. QCM-D measures the changes in the resonance frequency, Δf , and dissipation, ΔD , of a sensor crystal on interaction of soft matter with its surface. The QCM-D response is sensitive to the mass (including coupled water) and the mechanical properties of the surface-bound layer. Adsorption and interfacial processes were monitored *in situ* with sub-second time resolution, under continuous flow of sample solution. The thickness of FG repeat-domain monolayers was estimated by numerical fitting of the QCM-D data to a viscoelastic model.

Ellipsometry. Ellipsometry estimates the changes in the ellipsometric angles, Δ and ψ , of polarized light on reflection at a planar surface. We used ellipsometry *in situ*, using silicon wafers as substrates that were installed in an open cuvette with continuously stirred sample solution, to quantify adsorbed/absorbed masses in a time-resolved manner. Samples were injected directly into the cuvette and excess sample was removed by repeatedly diluting the cuvette content in buffer. Bound masses were determined by numerical fitting of the ellipsometric data.

Nanoindentation assays by AFM. Force–displacement curves were acquired by using Si₃N₄ probes with a nominal apex radius below 10 nm. The SLBs and FG repeat films were prepared on silicon wafers and probed in buffer with maximal loads of 1 nN.

Supplementary information is available at *EMBO reports* online (<http://www.emboreports.org>).

ACKNOWLEDGEMENTS

This study was supported financially by funds from the Department of Industry of the Basque Government (to N.E. and R.P.R.), the Max Planck Society, and Deutscher Akademischer Austausch Dienst (to N.E.).

CONFLICT OF INTEREST

The authors declare that they have no conflict of interest.

REFERENCES

Allen NPC, Huang L, Burlingame A, Rexach M (2001) Proteomic analysis of nucleoporin interacting proteins. *J Biol Chem* **276**: 29268–29274

Bednenko J, Cingolani G, Gerace L (2003) Importin- β contains a COOH-terminal nucleoporin binding region important for nuclear transport. *J Cell Biol* **162**: 391–401

Ben-Efraim I, Gerace L (2001) Gradient of increasing affinity of importin- β for nucleoporins along the pathway of nuclear import. *J Cell Biol* **152**: 411–417

Bingen P, Wang G, Steinmetz NF, Rodahl M, Richter RP (2008) Solvation effects in the QCM-D response to biomolecular adsorption—a phenomenological approach. *Anal Chem* **80**: 8880–8890

Denning DP, Patel SS, Uversky V, Fink AL, Rexach M (2003) Disorder in the nuclear pore complex: the FG repeat regions of nucleoporins are natively unfolded. *Proc Natl Acad Sci USA* **100**: 2450–2455

Frey S, Görlich D (2007) A saturated FG-repeat hydrogel can reproduce the permeability properties of nuclear pore complexes. *Cell* **130**: 512–523

Frey S, Görlich D (2009) FG/FxFG as well as GLFG repeats form a selective permeability barrier with self-healing properties. *EMBO J* **28**: 2554–2567

Isgro TA, Schulten K (2005) Binding dynamics of isolated nucleoporin repeat regions to importin- β . *Structure* **13**: 1869–1879

Lata S, Gavutis M, Piehler J (2006) Monitoring the dynamics of ligand–receptor complexes on model membranes. *J Am Chem Soc* **128**: 6–7

Lim RYH, Huang N-P, Köser J, Deng J, Lau KHA, Schwarz-Herion K, Fahrenkrog B, Aebi U (2006) Flexible phenylalanine–glycine nucleoporins as entropic barriers to nucleocytoplasmic transport. *Proc Natl Acad Sci USA* **103**: 9512–9517

Lim RY, Fahrenkrog B, Koser J, Schwarz-Herion K, Deng J, Aebi U (2007) Nanomechanical basis of selective gating by the nuclear pore complex. *Science* **318**: 640–643

Macara IG (2001) Transport into and out of the nucleus. *Microbiol Mol Biol Rev* **65**: 570–594

Mohr D, Frey S, Fischer T, Güttler T, Görlich D (2009) Characterisation of the passive permeability barrier of nuclear pore complexes. *EMBO J* **28**: 2541–2553

Peters R (2005) Translocation through the nuclear pore complex: selectivity and speed by reduction-of-dimensionality. *Traffic* **6**: 421–427

Peters R (2009) Translocation through the nuclear pore: Kaps pave the way. *Bioessays* **31**: 466–477

Pyhtila B, Rexach M (2003) A gradient of affinity for the karyopherin Kap95p along the yeast nuclear pore complex. *J Biol Chem* **278**: 42699–42709

Rabut G, Doye V, Ellenberg J (2004) Mapping the dynamic organization of the nuclear pore complex inside single living cells. *Nat Cell Biol* **6**: 1114–1121

Ribbeck K, Görlich D (2001) Kinetic analysis of translocation through nuclear pore complexes. *EMBO J* **20**: 1320–1330

Ribbeck K, Görlich D (2002) The permeability barrier of nuclear pore complexes appears to operate via hydrophobic exclusion. *EMBO J* **21**: 2664–2671

Richter RP, Bérat R, Brisson AR (2006) The formation of solid-supported lipid bilayers—an integrated view. *Langmuir* **22**: 3497–3505

Rout MP, Aitchison JD, Magnasco MO, Chait BT (2003) Virtual gating and nuclear transport: the hole picture. *Trends Cell Biol* **13**: 622–628

Strawn LA, Shen T, Shulga N, Goldfarb DS, Wentz SR (2004) Minimal nuclear pore complexes define FG repeat domains essential for transport. *Nat Cell Biol* **6**: 197–206

Yang Q, Rout MP, Akey CW (1998) Three-dimensional architecture of the isolated yeast nuclear pore complex: functional and evolutionary implications. *Mol Cell* **1**: 223–234



EMBO reports is published by Nature Publishing Group on behalf of European Molecular Biology Organization. This article is licensed under a Creative Commons Attribution-NonCommercial-Share Alike 3.0 License. [<http://creativecommons.org/licenses/by-nc-sa/3.0/>]